2-2017

Polyubiquitination of Apurinic/Apyrimidinic Endonuclease 1 by Parkin

Timothy L. Scott
University of Kentucky, tim.scott@uky.edu

Christina A. Wicker
University of Kentucky, christina.wicker@uky.edu

Rangaswamy Suganya
Houston Methodist Research Institute

Bithika Dhar
University of Kentucky, bdhar2@email.uky.edu

Thomas A. Pittman
University of Kentucky, thomas.pittman@uky.edu

See next page for additional authors

Authors
Timothy L. Scott, Christina A. Wicker, Rangaswamy Suganya, Bithika Dhar, Thomas A. Pittman, Craig Horbinski, and Tadahide Izumi

Polyubiquitination of Apurinic/Apyrimidinic Endonuclease 1 by Parkin

Notes/Citation Information
Published in *Molecular Carcinogenesis*, v. 56, issue 2, p. 325-336.

Digital Object Identifier (DOI)
https://doi.org/10.1002/mc.22495

HHS Public Access

Author manuscript

Mol Carcinog. Author manuscript; available in PMC 2018 February 01.

Published in final edited form as:

Mol Carcinog. 2017 February ; 56(2): 325–336. doi:10.1002/mc.22495.

Polyubiquitination of Apurinic/Apyrimidinic Endonuclease 1 by Parkin

Timothy L. Scott[1,†], **Christina A. Wicker**[1,†], **Rangaswamy Suganya**[2], **Bithika Dhar**[1], **Thomas Pittman**[3], **Craig Horbinski**[4], and **Tadahide Izumi**[1,*]

[1]Department of Toxicology and Cancer Biology, University of Kentucky

[2]Radiation Oncology, Houston Methodist Research Institute

[3]Department of Neurosurgery, Universtiy of Kentucky

[4]Departments of Pathology and Neurosurgery, Northwestern University

Abstract

Apurinic/apyrimidinic endonuclease 1 (APE1) is an essential protein crucial for repair of oxidized DNA damage not only in genomic DNA but also in mitochondrial DNA. Parkin, a tumor suppressor and Parkinson's disease (PD) associated gene, is an E3 ubiquitin ligase crucial for mitophagy. While DNA damage is known to induce mitochondrial stress, Parkin's role in regulating DNA repair proteins has not been elucidated. In this study, we examined the possibility of Parkin-dependent ubiquitination of APE1. Ectopically expressed APE1 was degraded by Parkin and PINK1 via polyubiquitination in mouse embryonic fibroblast cells. PD-causing mutations in Parkin and PINK1 abrogated APE1 ubiquitination. Interaction of APE1 with Parkin was observed by co-immunoprecipitation, proximity ligation assay, and co-localization in the cytoplasm. N-terminal deletion of 41 amino acid residues in APE1 significantly reduced the Parkin-dependent APE1 degradation. These results suggested that Parkin directly ubiquitinated N-terminal Lys residues in APE1 in the cytoplasm. Modulation of Parkin and PINK1 activities under mitochondrial or oxidative stress caused moderate but statistically significant decrease of endogenous APE1 in human cell lines including SH-SY5Y, HEK293, and A549 cells. Analyses of glioblastoma tissues showed an inverse relation between the expression levels of APE1 and Parkin. These results suggest that degradation of endogenous APE1 by Parkin occur when cells are stressed to activate Parkin, and imply a role of Parkin in maintaining the quality of APE1, and loss of Parkin may contribute to elevated APE1 levels in glioblastoma.

Keywords

DNA repair; APE1; ubiquitination; Parkin; glioblastoma

[*]Correspondence to: Tadahide Izumi, Graduate Center for Toxicology, University of Kentucky, 1095 V.A. Dr., Lexington KY 40536 USA, Phone: 859-257-6472, t.izumi@uky.edu.

[†]These authors contributed equally to this work.

Introduction

Oxidatively damaged DNA is primarily repaired by DNA base excision repair. In the mammalian DNA base excision repair pathway, apurinic/apyrimidinic (AP) endonuclease (APE1) incises DNA upstream of AP sites to generate single-strand breaks (SSBs) with 3′-OH termini for subsequent DNA repair synthesis reactions [1]. APE1 is shown to be essential during mouse embryonic development and is the only active AP-endonuclease in mammals. Studies also demonstrated that APE1 was indispensable for cultured cells [2,3], although recent studies demonstrated that cells derived from a B lymphocyte line could survive without APE1 [4,5]. APE1 also functions as a gene expression regulator by redoxically activating oncogenic and pro-survival transcription factors such as AP-1 and NF-κB, and is also involved in gene regulation necessary for calcium homeostasis [6,7]. Therefore, APE1 is a pro-survival multifunctional protein. Drug and radiation resistance of tumor tissues have been linked to increased APE1 expression [8–12].

APE1 is post-translationally modified by phosphorylation, acetylation, and ubiquitination [13–19]. APE1 was found to be ubiquitinated by MDM2 [20,21], the major p53 regulator [22,23]. However, APE1 ubiquitination was later observed in mouse embryonic fibroblast defective of MDM2 [20], implying existence of backup activities for APE1 ubiquitination other than MDM2. Meisenberg et al. identified UBR3 as another E3 ubiquitin ligase for APE1 [24].

Properly maintained mitochondrial membrane potential is critical to meet cellular energy demands through oxidative phosphorylation. Electron leaks from the respiratory chain complexes result in the generation of superoxide (O_2^-). The mitochondrial superoxide dismutase is extremely efficient in scavenging O_2^- [25], and thus cells at normal growth conditions maintain the oxidative stress at a manageable level. This status quo may be broken by exogenous reagents, genotoxic stresses, and gene mutations that impair mitochondria [26–28]. Damaged mitochondria elevate intracellular reactive oxygen species (ROS), and result in further impairment of mitochondria [29]. To avoid this vicious cycle, a salvaging process named mitophagy is initiated to break down damaged mitochondria and generate new mitochondria [30]. It is becoming apparent that mitophagy is modulated by DNA damage responses. Recent studies found that activation of poly(ADP-ribose) polymerase 1 (PARP1) by DNA strand breaks plays a pivotal role in the energy metabolism [31,32]. In the process of DNA repair, oxidative DNA damage are converted to DNA strand breaks as intermediate lesions [33]. The suppression of mitophagy by the activated PARP may be a self-feedback system during the repair of endogenous DNA damage. However, understanding the interplay among factors for mitophagy and DNA repair proteins is far from complete.

During mitophagy, proteins in damaged mitochondria are degraded via polyubiquitination, which is mainly carried out by Parkin, a RING domain-containing E3 ubiquitin ligase [34]. PINK1 (PTEN-induced-kinase 1) is a critical activator of Parkin [30,34]. PINK1 phosphorylates ubiquitin and Parkin [35–38], and recruits Parkin from cytoplasm to mitochondrial surfaces to facilitate ubiquitination of its target proteins such as mitofusin 2 (Mfn2), Miro, and VDAC1 [39,40]. Mutations in the Parkin and the PINK1 genes cause

mitochondrial degeneration and are associated with PD [30] and glioblastoma (GBM) [41,42].

Considering that Parkin expression is induced by p53 [43,44] which enhances APE1 ubiquitination [21], it is possible that Parkin ubiquitinates APE1. Moreover, a recent proteomics study for identifying Parkin's substrates and interacting proteins revealed APE1 as one of possible targets of Parkin [45]. These observations prompted us to investigate the activity of Parkin for APE1 ubiquitination. In this study, we investigated functional and physical interactions between APE1, Parkin, and PINK1.

Materials and Methods

DNA, Cell culture and transient transfection

All cDNAs in plasmid expression vectors used in this study are of humans. Expression vectors for YFP-Parkin (23955) and cMyc-PINK1 (13314) [46,47] were obtained from Addgene. Non-tagged wild-type (wt) PINK1 was then cloned by PCR amplification into pcDNA3.1 (Invitrogen). The full-length human Parkin and its specific E2 ligase UbcH7 were cloned for this study by PCR cloning from quick cDNA clone (Clontech) using Phusion Taq DNA polymerase (NEB) with appropriate primers synthesized (Integrated DNA Technology) into the pcDNA3.1Zeo(+) expression vector (Invitrogen). Mutations (R275W and C431F in Parkin and G309D in PINK1) were introduced by PCR subcloning. The pBi16, a mammalian expression vector with a flippase recognition target (FRT) site and a doxycycline (dox) inducible-dual promoter [48], is a generous gift from Dr. Grabczyk. The human Parkin and PINK1 cDNAs were cloned into pBi16 (named pBi16-PaPi, Supplemental Fig. S1) for inducing both proteins together with dox. All sequences of DNA amplified by PCR were confirmed by DNA sequencing (ACGT Inc. and GenScript Inc). MEF^{la}, a mouse embryonic fibroblast cells, deficient in mouse Ape1 (mApe1) and expressing hAPE1 was described previously for its extremely low APE1 expression [49]. The MEF^{la} cells were cultured in DMEM High Glucose medium (Hyclone) supplemented with 10% fetal bovine serum (Gemini Inc.), 1% penicillin/streptomycin, 1% L-glutamine (Hyclone). SH-SY5Y (a human neuroblastoma) and A549 (a human lung adenocarcinoma) were purchased from ATCC. The HEK293 derivative T-Rex 293 was purchased from Invitrogen. The T-Rex 293 cells were transfected with pBi16-PaPi and pOG44 expressing flippase (Flp). 293/pBI16-PaPi (293-PaPi) stable transfectants were selected with 150 μg/mL hygromycin. The 293-PaPi cells were plated on 60 mm dishes (1×10^6/dish). After overnight incubation, Parkin and PINK1 were induced with 2 μg/mL dox. At the same time, drugs indicated in the results were added in the culture medium, and together incubated for 16 h. Cells were then harvested for immunoblot analyses.

For transient transfection, cells were plated on 60 mm dishes at 4×10^5 - 1×10^6 and incubated for overnight. Lipofectamine 2000 (Invitrogen) was used for transfection using OptiMEM-I (Invitrogen) with the vendors' manual. PINK1 siRNA was purchased from Applied Biosystem. Introduction of siRNA was standardized for minimum cytotoxicity as the following method. Semi-confluent SH-SY5Y cells were suspended in the DMEM medium at 1×10^7 cells/mL, and mixed with 200 nM siRNA. Cell/siRNA suspensions in 0.1 cm cuvettes were then electroporated using ECM 830 square wave electroporation system (BTX) at

920V, 120 μF, 2 pulses at 0.1 sec interval. After 15 min at room temperature, cells were transferred to 100 mm dishes (Corning) containing DMEM complete media, and incubated for 72 h. When necessary, 10 μM carbonyl cyanide 3-chlorophenylhydrazone (CCCP) was added after 48 h, and further incubated for 24 h (total 72 h after the electroporation). Cells were then harvested and examined with immunoblot.

Immunoblot (Western blot) assay

Whole cell extracts were prepared from cells detached by scraping after being washed with PBS twice, and resuspended in RIPA buffer [50] supplemented with proteinase inhibitor cocktail (Roche) and 40 μM MG132. After adjusting protein concentration, the extracts were run in 10% acrylamide SDS-PAGE, transferred to PVDF membrane (Bio-Rad), and blotted with appropriate antibodies. SDS-PAGE samples were run with a pre-stained protein size marker (NEB, P7709).

Detection of ubiquitinated APE1 in A549

Histidine hexamer-tagged ubiquitin (6xHis-ub) cDNA was transfected with APE1, Parkin, and PINK1 in A549 cells and incubated for 24 h. The cells were lysed in the binding buffer (20 mM Tris pH 8.0, 0.5 M NaCl, 0.1 % NP-40, 10 mM imidazole) with 40 μM MG132 (Sigma) and proteinase inhibitor cocktail without EDTA (Roche). The crude cell extracts (total fraction) were incubated with Ni-NTA magnetic beads (Qiagen) for 15 min at 4 °C, washed with the binding buffer, and eluted with binding buffer with 120 mM imidazole. The total and eluted (His-tagged protein-enriched) fractions were analyzed by immunoblot using anti-APE1 antibody.

Analysis of localization of YFP-Parkin and APE1

MEF^{la} cells were spread on coverslips a day before DNA transfection. The cDNA carrying YFP-Parkin and APE1 were co-transfected in the same way as described above, and incubated for 24 h. If necessary, MG132 was added and incubated. Cells were incubated in the presence of Mitotracker Red (Invitrogen), fixed in 3.7% formaldehyde, and then permeabilized in PBS containing 0.2% TritonX-100 for 15 min. After washing with PBS twice, cells were blotted with anti-APE1 antibody, stained with anti-mouse IgG antibody conjugated to Alexa Fluor 488 (Invitrogen) followed by DAPI staining, and mounted on glass plates with Vector Lab mounting reagent. Cells were then analyzed with Leica TSP SP5 Confocal Microscope confocal microscopy at the Imaging Core facility of University of Kentucky.

Co-immunoprecipitation (co-IP) of recombinant APE1-FLAG and Parkin

E. coli BLR(DE3) strain (EMD Biosciences) was transformed with a pRSF-Duet1 derivative (EMD) carrying Parkin and either of APE1-FLAG or APE1 (negative control) cDNAs. The cells were grown until OD600 reached 0.6 to 0.8, and then expressions of the proteins were induced with 0.5 mM IPTG (Fisher) at 16°C for 16 h [20,51]. Cells were lysed in a co-IP buffer (120 mM NaCl, 2mM EDTA, 0.1mM EGTA, 0.05% NP40, 1 mM DTT, 50mM HEPES pH 7.9) supplemented with proteinase inhibitor cocktail (Complete Ultra Mini, Roche). After centrifugation for 20 min at 4°C, small portions of supernatants were kept

separately as total fractions (inputs), and the remaining samples were subjected to immunoprecipitation with agarose resin conjugated to the anti-FLAG antibody M2 (Sigma). The resin was washed in the co-IP buffer, and eluted in 100 μg/mL FLAG peptide (Sigma), and both total and IP fractions were analyzed by immunoblotting using anti-APE1 and anti-Parkin antibodies.

Proximity Ligation Assay (PLA)

A549 cells were spread on coverslips and incubated for overnight before transfection of the APE1 and Parkin cDNA. The cells were then incubated with 1 μM Mitotracker RED for 1 h, and fixed in 100% methanol at −20°C and then in 100% ice-cold acetone.

The samples were processed according to the OLINK Bioscience DuoLink In Situ protocol. Briefly, the coverslips were rehydrated in PBS (pH7.5) containing 0.1% Triton X-100 (v/v) for at least 30 minutes at room temperature. The samples were then blocked with 5% BSA in PBS+ Triton X-100 for 30 minutes. The primary antibodies were applied (1:200 ms-anti-parkin, 1:250 rb-anti-APE1) and incubated overnight at 4°C in a humidity chamber; all other incubations were carried out in a 37°C humidity chamber unless otherwise noted. The samples were washed and incubated with the Duolink secondary antibodies (anti-mouse and anti-rabbit IgG) for 1 hour. After washing, the samples were incubated with the ligation reaction mixture for 30 minutes, washed, and then further incubated with the green amplification reagent for 90 minutes. After the final wash, the samples were mounted with Duolink In Situ mounting medium containing DAPI. The fluorescent signals in the cells were analyzed using an Olympus inverted fluorescence microscope.

Tissue extract preparation

Snap-frozen GBM specimens were obtained from male patients (50–75 years old) in accordance with IRB regulations. Whole cell lysates of the tissues were prepared using the Fisher Cryo-homogenizing system. Briefly, the samples were disaggregated through grinding with a clean pre-chilled mortar and pestle. The samples were then transferred to a micro-centrifuge tube and RIPA buffer, containing 40 μM MG132 and protease inhibitors, was added to an approximate concentration of 10 mg/μL pre-ground weight. The samples were then centrifuged to collect large debris, and the supernatant was used to prepare a stock in SDS-PAGE loading buffer and to determine final protein concentration. The SDS-PAGE stock was sonicated and incubated at 70° C for 5 min and stored at −80° C until use. Before SDS-PAGE, the samples were diluted to a final concentration of 3 μg/μL in SDS-PAGE loading buffer.

Immunohistochemistry for GBM and control tissues

A combined total of 17 GBMs and control brain tissues were obtained from the Markey Cancer Center Biospecimen and Tissue Procurement Shared Resource Facility (BSTP SRF). Formal-dahydefixed paraffin embedded 5 μm sections were deparaffinized in xylene and rehydrated stepwise using graded ethanol and finally water. Dako antigen retrieval buffer was used with a Biocare Medical decloaking chamber for antigen retrieval following the manufacturer’s protocol. Dako peroxidase blocking reagent was used to inhibit endogenous peroxidase activity. Sections were incubated with primary antibody for 1 hour at room

temperature: APE1, Parkin. Next, sections were incubated with polymer linked secondary antibody, either mouse (Dako K4007) or rabbit (Dako K4003) for 30 min at room temperature followed by development with diaminobenzodine. Following washing, slides were counterstained with Meyer's hematoxylin and allowed to Blue in Ammonia water before dehydration in graded ethanol. Slides were incubated in xylene before affixing coverslip.

High-resolution digital image slides of GBM and control brain tissue were obtained by scanning with the Aperio ScanScope (Leica) at 20x magnification. Aperio ImageScope software V 11.2.0.780 and the software's algorithms for Positive Pixel Count V9 and Nuclear V9 were used to analyze these images for % total intensities for APE1 and Parkin in tissue and nuclear localization respectively.

Chemicals and other reagents

CCCP and MG132 were purchased from Sigma. Antibodies used in this study are those for APE1 (Santa Cruz, sc-55498), PINK1 (Novus BC100-494 and Protein Tech 23274-1-AP), Parkin (Santa Cruz, sc-32282), β-tubulin (Santa Cruz, sc58884), GAPDH (Invitrogen, AM4300), p53 (Santa Cruz, sc-126). Pre-stained protein molecular weight marker was purchased from New England Biolab (P7709).

Results

Direct involvement of Parkin in APE1 ubiquitination

To test whether APE1 is ubiquitinated by Parkin, protein extracts from A549 expressing histidine hexamer-tagged ubiquitin (His-Ub), APE1, Parkin and PINK1 were subjected to enrichment of His-Ub through nickel resin purification [21]. Monoubiquitinated as well as polyubiquitinated APE1 were detected in the His-Ub enriched fraction when Parkin was expressed (Fig. 1A lane 2 v.s. lane 1). The results indicated Parkin was capable of ubiquitinating APE1. The His-Ub diminished when PINK1 was co-expressed while intact APE1 decreased (lane 3 v.s. lane 4), suggesting that PINK1 was required for polyubiquitination and degradation of APE1.

To understand functional requirements of Parkin and PINK1 for APE1 ubiquitination, a mouse embryonic fibroblast cell line MEF^{la} ($MEF^{lowAPE1}$) [49] was transiently transfected with Parkin, PINK1, and APE1. APE1 levels were not altered when either Parkin or PINK1 was expressed alone (Fig. 1B lanes 3 and 4 v.s. lane 2). However, expressing both Parkin and PINK1 caused a marked APE1 decrease (Fig. 1B lane 5; also in Fig. 1D lane 3, Fig. 1E lane 3E, and Fig. 1F lane 2).

p53 is a well known target of ubiquitination by other E3 ubiquitin ligases [52–54]. We tested whether p53 was also efficiently ubiquitinated by Parkin. However, the stability of p53 was unaffected by Parkin and PINK1 (Fig. 1C). Similarly, proliferating cell nuclear antigen (PCNA), highly susceptible to mono- and poly-ubiquitination [54], was not modified by Parkin (Fig. 1C). The unaltered stabilities of p53 and PCNA as well as β-tubulin and β-actin indicated a high specificity of the reaction of Parkin on APE1. Incubating cells with a 26S proteasome inhibitor MG132 restored the APE1 level (Fig. 1D, lane 4 v.s. lane 3).

The Parkin polypeptide contains two RING domains (Fig. S2). R275W and C431F missense mutations, which are located in the first and second RING domains in Parkin respectively (Fig. S2), abrogate its E3 ligase activity and cause early onset PD [39,55]. These Parkin mutants failed to degrade APE1 (Fig. 1D lanes 5 and 9; Table 1). PINK1 carrying G309D missense mutation is defective in its kinase activity (Fig. S2), and incapable of activating Parkin [47,56,57]. The G309D PINK1 did not activate APE1 degradation (Fig. 1D lane 6; Table 1). These results suggested that the ligase activity of Parkin was required for APE1 degradation, for which the kinase activity of PINK1 was also critical.

Interaction of APE1 with Parkin

Sarraf et al. recently identified proteins interacting with Parkin and their possible ubiquitination sites, and APE1 was found to be a protein interacting with Parkin through its N-terminal segment, i.e., 20–30th amino acids from N-terminus [45]. To probe the importance of the N-terminal region of APE1 for the stability, MEF^{la} cells were transiently transfected with N-terminally truncated APE1, ND20 and ND41 (N-terminal 20 and 41 amino acids deletions), along with Parkin and PINK1. While ND20 APE1 was efficiently degraded by Parkin (Fig. 1E and Table 1), ND41 APE1 was significantly more resistant to Parkin dependent degradation compared to those of the full-length and ND20 APE1 (Fig. 1F and Table 1). It is likely that APE1 is mainly ubiquitinated at the amino acid residues 20–41 which contains two Lys clusters (24K-25K-27K and 31K-32K-35K), which is consistent with the previous studies showing that the N-terminal residues contained major ubiquitin acceptor Lys residues catalyzed by MDM2 and UBR3 [21,24].

In the normal condition, APE1 in MEF^{la} was localized predominantly in the nuclei (Fig. 2A, control). When the cells were treated with MG132, cytoplasmic APE1 was visibly increased 3 h after the treatment, and became indistinguishable from the nuclear APE1 after overnight incubation of the cells with MG132 (Fig. 2A). The major fraction of Parkin is present in the cytoplasm [40]. The possibility of cytosolic co-localization of APE1 with Parkin was elucidated, using YFP-Parkin and APE1. After MG132 treatment, APE1 was found to be co-localized with YFP-Parkin in the cytoplasm (Fig. 2B **and** Fig. S3). The cytoplasmic co-localization of APE1 and YFP-Parkin suggested that the physical interaction occurred in the cytoplasm. This possibility was examined with proximity ligation assay (PLA) [58]. Antibodies specific to APE1 and Parkin were used to label the two proteins and signals were detected when the two proteins were in the proximate location to each other (Fig. 2C). The PLA signal was detected when APE1 and Parkin were co-expressed. Importantly, the PLA was observed mainly in the cytoplasm but not in the nuclei or inside of mitochondria. The absence of Parkin-APE1 interaction in the nuclei is consistent with the cytosolic localization of Parkin in previous studies [59–61]. To test whether APE1 directly interacts with Parkin without involvement of other cellular factors such as ubiquitin or PINK1, recombinant Parkin was expressed with APE1 or with FLAG-APE1 simultaneously in *E. coli*, and performed FLAG-immunoprecipitation to detect Parkin in the FLAG-APE1 enriched fraction. Parkin was specifically detected in the FLAG-APE1 containing fraction (Fig. 2D). The result indicated that APE1 directly interacts with Parkin. Co-immunoprecipitation of Parkin by ND41 APE1-FLAG was significantly decreased (Fig. S4) compared to that by full-length APE1, indicating that the N-terminal segment is pivotal for the interaction.

However, it should be noted that Parkin signal was not completely disappeared in the ND41-FLAG IP fraction, and we could not exclude the possibility that the downstream APE1 polypeptide is also involved in the interaction of APE1 with Parkin.

Ubiquitination and degradation of endogenous APE1 by Parkin and PINK1

To examine the effect of Parkin expression on endogenous APE1, a lung adenocarcinoma cell line A549 was transiently co-transfected with Parkin and its cofactors [39] [62–65], namely, Uba1 (E1 ligase), UbcH7 (Parkin-specific E2 ligase), and PINK1 (Fig. 3A). The level of endogenous APE1 decreased in a does-dependent manner (Fig. 3B). Densitometry of the immunoblot revealed that the level of the endogenous APE1 was down to 60% of the control cells transfected with the vector plasmid DNA alone.

Levels of the endogenous p53 and PCNA as well as housekeeping proteins β-tubulin and GAPDH were unaltered by the expression of Parkin and its cofactors (Fig. 3B). These results indicated a high specificity of the reaction of Parkin on APE1, consistent with the results with the ectopically expressed proteins (Fig. 1C). Total protein extracts from A549 were analyzed for ubiquitination of endogenous APE1. A specific band appeared at the position for monoubiquitinated APE1 after cells were transiently transfected with Parkin (Fig. 3C). Therefore, endogenous APE1 was ubiquitinated and degraded by Parkin.

Inducible expression of Parkin and PINK1 without transient transfection would provide a more refined experimental condition. To achieve this, a derivative of HEK 293 cell line 293-PaPi was used. The 293-PaPi is a stable transfectant of HEK293, and enables simultaneous induction of Parkin and PINK1 by doxycycline from a bidirectional promoter [48] (Fig. S1). Induction of Parkin and PINK1 (Fig. 4A) did not alter APE1 nor β-tubulin while Mfn2 decreased clearly (Fig. 4B). Because Parkin's E3 ligase function is active at mitochondria, the 293-PaPi cells were treated with H_2O_2 to increase APE1 in mitochondria [66]. Treatment of the cells with H_2O_2 decreased APE1 to approximately 70% of the control while the amount of β-tubulin was still unchanged (Fig. 4B). Although the change of APE1 level by H_2O_2 in the dox-treated 293-PaPi was statistically significant, dox or H_2O_2 alone did not show significant difference from the untreated control cells (Fig. 4B). These results indicated that degradation of APE1 by Parkin was limited compared to the transiently expressed APE1, suggesting that a large portion of APE1 is not in contact with the Parkin and PINK1 without induction of stresses such as oxidative stress.

A human neuroblastoma cell line SH-SY5Y has been used for mitophagy studies because of a relatively high level of endogenous Parkin in the cells. SH-SY5Y cells were incubated with CCCP and the APE1 stability was examined. CCCP is a proton ionophore uncoupling oxidative phosphorylation in mitochondria [67] and stimulates mitophagy via Parkin-driven degradation of mitochondrial proteins 24 h after CCCP treatment [40]. Mitofusin 2 (Mfn2), a mitochondria fusion protein and a known Parkin substrate, was decreased after the CCCP treatment (Fig. 4C). The CCCP treatment also decreased the Parkin level, consistent with previous observations that Parkin polyubiquitinates itself for degradation as an auto-feedback regulation [68,69]. Under this condition, moderate decrease of APE1 was observed whereas the level of β-tubulin was unchanged. After normalization with β-tubulin, it was calculated, with statistical significance, that APE1 decreased to 80% of that of untreated

cells (Fig. 4C). The differentiation status of the SH-SY5Y [70] cells did not affect the Parkin activity, as cells that were differentiated with retinoic acid also showed a similar level of decrease of endogenous APE1 with CCCP (Fig. 4C). PINK1 down-regulation by RNA interference resulted in the stabilization of APE1 (Fig. 4D). These results suggested that Parkin and PINK1 played a role in regulating APE1 levels in the cells.

Loss of Parkin is associated with elevated APE1 levels in GBM

Parkin deficiency has been associated with GBM [41,42]. To elucidate the correlation between Parkin and APE1 in brain tumors, expression levels of Parkin and APE1 in both GBM and non-neoplastic brain tissues were examined. Qualities of the monoclonal antibodies for Parkin and APE1 were confirmed in Western blot to detect the corresponding proteins specifically (Fig. 5A). Interestingly, the GBM tissues showed increased APE1 levels while decreasing the Parkin levels (Fig. 5A). Parkin and APE1 levels were examined in detail by immunohistochemistry (Fig. 5B). Parkin levels in the non-neoplastic brain tissues were higher than those of GBM tissues (Fig. 5C, $p = 0.0009$), while APE1 signals were higher in GBM tissues than the non-neoplastic tissues ($p = 0.0025$). Parkin/APE1 ratios were calculated, and were significantly lower in the GBM tissues than in the non-neoplastic brain tissues (Fig. 5C, $p = 0.0013$). Notably, the variance of Parkin/APE1 ratios were significantly lower than that of either APE1 and Parkin levels, implying that the loss of Parkin and the gain of APE1 expression during the tumorigenesis are associated with each other.

Discussion

APE1 is primarily known for repair of oxidized and alkylated DNA damage, but also is an important gene expression regulator that activates transcription factors such as AP-1 and NFκB [71]. Both APE1 functions are pro-proliferation and advantageous to cell survival, which explains elevated APE1 expression in tumor tissues. Indeed, tumor cells with high APE1 levels acquire drug and radiation resistance [8–12]. Therefore, identifying factors that control APE1 levels should provide information relevant to the cancer therapeutics, particularly those causing cyto-toxicity via DNA damage generation.

We speculated a possible role of Parkin for controlling intracellular levels of APE1, because (1) backup E3 ligase activity was detected in cells defective in MDM2 [20], (2) Parkin is induced by p53 [43,44], and (3) a proteomics study detected APE1 as a possible substrate of Parkin [45]. The present results show that Parkin is a quite efficient and highly specific E3 ligase to ubiquitinate APE1. The examination of mutant Parkin and PINK1 supports that the ubiquitination reaction is dependent on the E3 ligase activity of Parkin and the kinase activity of PINK1. Evidence for the direct interaction of APE1 with Parkin was obtained with co-immunoprecipitation of APE1 and Parkin and by proximity ligation assay. Based on these results, we conclude that Parkin directly ubiquitinates APE1. While monoubiquitinated APE1 was readily detected by MDM2 and UBR3 [21,24], detection of monoubiquitinated APE1 catalyzed by Parkin and PINK1 was relatively difficult. This observation implies that monoubiquitinated APE1 immediately undergoes polyubiquitination process by Parkin, and APE1 is efficiently degraded after the reaction by Parkin. Inhibiting the 26S proteasome by MG132 resulted in increase of monoubiquitinated APE1 in a manner dependent on Parkin

and PINK1. Thus, Parkin with its cofactors Uba1, UbcH7, and PINK1 ubiquitinates directly, and degrades APE1 through 26S proteasome more efficiently than those processed by MDM2 and UBR3.

While ND20 APE1 (N-terminal 20 a.a. truncation) was degraded by Parkin as effectively as the full-length APE1, the stability of ND41 APE1 in the presence of Parkin and PINK1 was significantly increased. The results indicated that the N-terminal polypeptide between 20 to 40 amino residues in APE1 is important for the Parkin-dependent ubiquitination.

The N-terminal 60 amino acid segment in APE1 is not defined well functionally and structurally. This domain is unique in the mammalian AP endonuclease [72], and is dispensable for the AP-endonuclease activity [73], and thus it has been speculated that the N-terminal domain has an uncharacterized function unique to mammalian cells. In this context, it is interesting that the segment is rich in Lys, the major acceptor for acetylation and ubiquitination. The N-terminal segment between 20 and 41 amino acid residues contains six Lys residues, namely, 24K, 25K, 27K, 31K, 32K, and 35K. Acetylation of APE1 at these Lys residues were reported [7,14,18,74]. These N-terminal Lys residues were also the main ubiquitin acceptors for MDM2 and UBR3 E3 ligases [21,24]. Based on a recent quantitative proteomics study, the APE1 segment 18-RTEPEAKKSKTAA-30, containing Lys 24, 25 and 27, was identified to be a possible target of ubiquitination catalyzed by Parkin [45]. Therefore, Lys residues in the N-terminus may be essential for the post-translational modifications that modulates APE1's gene regulatory function [7] and for altering its stability by polyubiquitination.

Although activating Parkin resulted in decrease of endogenous APE1 in three cell lines, SH-SY5Y, A549, and 293-PaPi, it should be noted that Parkin was active on endogenous APE1 only when stressful conditions (CCCP and H_2O_2) were invoked. We speculate that the modest effect of Parkin on endogenous APE1 is due to the fact that the majority of endogenous APE1 is compartmentalized in the nuclei, which may prevent Parkin from reacting on APE1. Stresses induced in the cells activated Parkin system (CCCP in SH-SY5Y) or facilitated mitochondrial localization of APE1 from nuclei (H_2O_2 in 293) [66]. Although endogenous APE1 significantly decreased in A549 without any treatments, transient transfection is known to induce stress responses [75,76]. Thus, APE1 ubiquitination by Parkin is unique in that the main site of the reaction is the cytoplasm, which is supported by the proximity ligation assay. In contrast, APE1 ubiquitination by MDM2 and UBR3 occurred mainly in the nuclei [20,24]. It should be noted that APE1 was co-purified with mitochondria, but majority of this APE1 fraction was found to be on the surface of mitochondria [77], which is the major platform for the Parkin driven protein degradation. However, it is highly plausible in the event of mitophagy, APE1 in the mitochondria becomes the target of Parkin as well.

While APE1 has been studied for its activities in the nuclei, there is an increasing interest in APE1's presence in the cytoplasm and its cancer-promoting effect [78–80]. Kakolyris et al. found that APE1 was present in the cytoplasm of the normal human tissues [81]. More recently, malignant cancer cells in the lung exhibited cytoplasmic APE1 at unusually high levels, and was linked to a poor prognosis of cancer treatment [79]. Vascott et al. found that

treatment of cells with an APE1 inhibitor E3330 caused cytoplasmic translocation of APE1 [82]. Frossi also found that H_2O_2 induced translocation of APE1 into mitochondria [66]. These studies suggest a cellular mechanism to export APE1 from nuclei. Based on these previous studies and present results, it is postulated that APE1 ubiquitination by Parkin is active in the cytoplasm, in which damaged APE1 proteins are ubiquitinated and degraded by Parkin to protect cells from undergoing malignant transformation. Meanwhile, undamaged, properly folded APE1 in the nucleus may be protected from this salvage system by the compartmentalization.

Originally identified as a gene of which deficiency is responsible for PD, Parkin was recently reported as a tumor suppressor gene of which loss of heterozygosity was frequently found in GBM [41]. Analysis of Parkin and APE1 expressions in normal and GBM specimens revealed that Parkin/APE1 ratios (expression of Parkin relative to that of APE1) in the GBM tissues were uniformly low, while those in the non-neoplastic brain tissues showed much higher values and larger variance than those in GBM. This observation implies a correlation between the loss of Parkin and the high expression of APE1 in the brain tumor tissues. It is possible that a lack of Parkin activity either by loss of heterozygosity or by p53 mutation may lead to deficiency in regular APE1 degradation, and may accumulate in the cytoplasm as well as in the nuclei. However, the results do not determine whether Parkin deficiency is the direct cause of high APE1 activities in GBM, or vice versa. More recently, Hu et al. reported that melanoma specific inactivation of the Parkin gene [83]. According to the study, melanoma specific Parkin alterations were observed at significantly high odds ratios over healthy control tissues The alterations included copy number variations, splicing mutations, and putatively inactivating mutations including N273S, R275W, and P437L which are adjacent to the missense mutations that cause early onset Parkinson’s disease (R275W and C431F). Further studies are necessary to investigate whether Parkin is crucial for the tight regulation of the intracellular level and subcellular distribution of APE1 to prevent cells from becoming malignant tumors.

Supplementary Material

Refer to Web version on PubMed Central for supplementary material.

Acknowledgments

This study was supported by NCI grant CA098664 (T.I.) and Cancer Center Supporting Grant (P30CA17758) by the Markey Cancer Center at University of Kentucky. We thank Dr. E. Grabczyk for his providing the pBi16 vector and acknowledge D. Napier’s expertise on the immunohistochemisty which was crucial for this study. We would like to thank Ms. Chawsheen and Martínez-Traverso for their technical assistance.

Abbreviations

AP-site	apurinic/apyrimidinic site
APE1	AP-endonuclease 1
CCCP	Carbonyl cyanide 3-chlorophenylhydrazone
co-IP	co-immunoprecipitation

dox	doxycycline
GBM	glioblastoma multiform
His-Ub	histidine hexamer-tagged ubiquitin
MDM2	mouse double minute 2
MEF	mouse embryonic fibroblast
PCNA	proliferating cell nuclear antigen
PINK1	PTEN induced kinase 1
PLA	proximity ligation assay
PTM	post-translational modification
wt	wild-type
YFP	yellow fluorescence protein

References

1. Izumi T, Wiederhold LR, Roy G, et al. Mammalian DNA base excision repair proteins: their interactions and role in repair of oxidative DNA damage. Toxicology. 2003; 193(1–2):43–65. [PubMed: 14599767]
2. Fung H, Demple B. A vital role for Ape1/Ref1 protein in repairing spontaneous DNA damage in human cells. Mol Cell. 2005; 17(3):463–470. [PubMed: 15694346]
3. Izumi T, Brown DB, Naidu CV, et al. Two essential but distinct functions of the mammalian abasic endonuclease. Proc Natl Acad Sci U S A. 2005; 102(16):5739–5743. [PubMed: 15824325]
4. Masani S, Han L, Yu K. Apurinic/apyrimidinic endonuclease 1 is the essential nuclease during immunoglobulin class switch recombination. Mol Cell Biol. 2013; 33(7):1468–1473. [PubMed: 23382073]
5. Xu J, Husain A, Hu W, Honjo T, Kobayashi M. APE1 is dispensable for S-region cleavage but required for its repair in class switch recombination. Proc Natl Acad Sci U S A. 2014; 111(48): 17242–17247. [PubMed: 25404348]
6. Tell G, Quadrifoglio F, Tiribelli C, Kelley MR. The many functions of APE1/Ref-1: not only a DNA repair enzyme. Antioxid Redox Signal. 2009; 11(3):601–620. [PubMed: 18976116]
7. Bhakat KK, Mantha AK, Mitra S. Transcriptional regulatory functions of mammalian AP-endonuclease (APE1/Ref-1), an essential multifunctional protein. Antioxid Redox Signal. 2009; 11(3):621–638. [PubMed: 18715144]
8. Bobola MS, Blank A, Berger MS, Stevens BA, Silber JR. Apurinic/apyrimidinic endonuclease activity is elevated in human adult gliomas. Clin Cancer Res. 2001; 7(11):3510–3518. [PubMed: 11705870]
9. Bobola MS, Finn LS, Ellenbogen RG, et al. Apurinic/apyrimidinic endonuclease activity is associated with response to radiation and chemotherapy in medulloblastoma and primitive neuroectodermal tumors. Clin Cancer Res. 2005; 11(20):7405–7414. [PubMed: 16243814]
10. Silber JR, Bobola MS, Blank A, et al. The apurinic/apyrimidinic endonuclease activity of Ape1/Ref-1 contributes to human glioma cell resistance to alkylating agents and is elevated by oxidative stress. Clin Cancer Res. 2002; 8(9):3008–3018. [PubMed: 12231548]
11. Curtis CD, Thorngren DL, Nardulli AM. Immunohistochemical analysis of oxidative stress and DNA repair proteins in normal mammary and breast cancer tissues. BMC Cancer. 2010; 10:9. [PubMed: 20064251]

12. Koukourakis MI, Giatromanolaki A, Kakolyris S, et al. Nuclear expression of human apurinic/apyrimidinic endonuclease (HAP1/Ref-1) in head-and-neck cancer is associated with resistance to chemoradiotherapy and poor outcome. Int J Radiat Oncol Biol Phys. 2001; 50(1):27–36. [PubMed: 11316543]
13. Yacoub A, Kelley MR, Deutsch WA. The DNA repair activity of human redox/repair protein APE/Ref-1 is inactivated by phosphorylation. Cancer Res. 1997; 57(24):5457–5459. [PubMed: 9407949]
14. Lirussi L, Antoniali G, Vascotto C, et al. Nucleolar accumulation of APE1 depends on charged lysine residues that undergo acetylation upon genotoxic stress and modulate its BER activity in cells. Mol Biol Cell. 2012; 23(20):4079–4096. [PubMed: 22918947]
15. Fritz G, Kaina B. Phosphorylation of the DNA repair protein APE/REF-1 by CKII affects redox regulation of AP-1. Oncogene. 1999; 18(4):1033–1040. [PubMed: 10023679]
16. Huang E, Qu D, Zhang Y, et al. The role of Cdk5-mediated apurinic/apyrimidinic endonuclease 1 phosphorylation in neuronal death. Nat Cell Biol. 2010; 12(6):563–571. [PubMed: 20473298]
17. Bhakat KK, Izumi T, Yang SH, Hazra TK, Mitra S. Role of acetylated human AP-endonuclease (APE1/Ref-1) in regulation of the parathyroid hormone gene. EMBO J. 2003; 22(23):6299–6309. [PubMed: 14633989]
18. Yamamori T, DeRicco J, Naqvi A, et al. SIRT1 deacetylates APE1 and regulates cellular base excision repair. Nucleic Acids Res. 2010; 38(3):832–845. [PubMed: 19934257]
19. Busso CS, Lake MW, Izumi T. Posttranslational modification of mammalian AP endonuclease (APE1). Cell Mol Life Sci. 2010; 67(21):3609–3620. [PubMed: 20711647]
20. Busso CS, Wedgeworth CM, Izumi T. Ubiquitination of human AP-endonuclease 1 (APE1) enhanced by T233E substitution and by CDK5. Nucleic Acids Res. 2011; 39(18):8017–8028. [PubMed: 21727086]
21. Busso CS, Iwakuma T, Izumi T. Ubiquitination of mammalian AP endonuclease (APE1) regulated by the p53-MDM2 signaling pathway. Oncogene. 2009; 28(13):1616–1625. [PubMed: 19219073]
22. Clegg HV, Itahana Y, Itahana K, Ramalingam S, Zhang Y. Mdm2 RING mutation enhances p53 transcriptional activity and p53-p300 interaction. PLoS One. 2012; 7(5):e38212. [PubMed: 22666487]
23. Itahana K, Mao H, Jin A, et al. Targeted inactivation of Mdm2 RING finger E3 ubiquitin ligase activity in the mouse reveals mechanistic insights into p53 regulation. Cancer Cell. 2007; 12(4):355–366. [PubMed: 17936560]
24. Meisenberg C, Tait PS, Dianova, et al. Ubiquitin ligase UBR3 regulates cellular levels of the essential DNA repair protein APE1 and is required for genome stability. Nucleic Acids Res. 2012; 40(2):701–711. [PubMed: 21933813]
25. Dhar SK, St Clair DK. Manganese superoxide dismutase regulation and cancer. Free Radic Biol Med. 2012; 52(11–12):2209–2222. [PubMed: 22561706]
26. Mouchiroud L, Houtkooper RH, Moullan N, et al. The NAD(+)/Sirtuin Pathway Modulates Longevity through Activation of Mitochondrial UPR and FOXO Signaling. Cell. 2013; 154(2):430–441. [PubMed: 23870130]
27. Houtkooper RH, Mouchiroud L, Ryu D, et al. Mitonuclear protein imbalance as a conserved longevity mechanism. Nature. 2013; 497(7450):451–457. [PubMed: 23698443]
28. Ohsawa S, Sato Y, Enomoto M, Nakamura M, Betsumiya A, Igaki T. Mitochondrial defect drives non-autonomous tumour progression through Hippo signalling in Drosophila. Nature. 2012; 490(7421):547–551. [PubMed: 23023132]
29. Kazak L, Reyes A, Holt IJ. Minimizing the damage: repair pathways keep mitochondrial DNA intact. Nat Rev Mol Cell Biol. 2012; 13(10):659–671. [PubMed: 22992591]
30. Youle RJ, Narendra DP. Mechanisms of mitophagy. Nat Rev Mol Cell Biol. 2011; 12(1):9–14. [PubMed: 21179058]
31. Fouquerel E, Goellner EM, Yu Z, et al. ARTD1/PARP1 negatively regulates glycolysis by inhibiting hexokinase 1 independent of NAD+ depletion. Cell Rep. 2014; 8(6):1819–1831. [PubMed: 25220464]
32. Fang EF, Scheibye-Knudsen M, Brace LE, et al. Defective mitophagy in XPA via PARP-1 hyperactivation and NAD(+)/SIRT1 reduction. Cell. 2014; 157(4):882–896. [PubMed: 24813611]

33. Hegde ML, Izumi T, Mitra S. Oxidized base damage and single-strand break repair in Mammalian genomes: role of disordered regions and posttranslational modifications in early enzymes. Prog Mol Biol Transl Sci. 2012; 110:123–153. [PubMed: 22749145]
34. Pickrell AM, Youle RJ. The Roles of PINK1, Parkin, and Mitochondrial Fidelity in Parkinson's Disease. Neuron. 2015; 85(2):257–273. [PubMed: 25611507]
35. Koyano F, Okatsu K, Kosako H, et al. Ubiquitin is phosphorylated by PINK1 to activate parkin. Nature. 2014; 510(7503):162–166. [PubMed: 24784582]
36. Wauer T, Swatek KN, Wagstaff JL, et al. Ubiquitin Ser65 phosphorylation affects ubiquitin structure, chain assembly and hydrolysis. EMBO J. 2015; 34(3):307–325. [PubMed: 25527291]
37. Kane LA, Lazarou M, Fogel AI, et al. PINK1 phosphorylates ubiquitin to activate Parkin E3 ubiquitin ligase activity. J Cell Biol. 2014; 205(2):143–153. [PubMed: 24751536]
38. Kazlauskaite A, Kondapalli C, Gourlay R, et al. Parkin is activated by PINK1-dependent phosphorylation of ubiquitin at Ser65. Biochem J. 2014; 460(1):127–139. [PubMed: 24660806]
39. Wang X, Winter D, Ashrafi G, et al. PINK1 and Parkin target Miro for phosphorylation and degradation to arrest mitochondrial motility. Cell. 2011; 147(4):893–906. [PubMed: 22078885]
40. Geisler S, Holmstrom KM, Skujat D, et al. PINK1/Parkin-mediated mitophagy is dependent on VDAC1 and p62/SQSTM1. Nat Cell Biol. 2010; 12(2):119–131. [PubMed: 20098416]
41. Veeriah S, Taylor BS, Meng S, et al. Somatic mutations of the Parkinson's disease-associated gene PARK2 in glioblastoma and other human malignancies. Nat Genet. 2010; 42(1):77–82. [PubMed: 19946270]
42. Gong Y, Zack TI, Morris LG, et al. Pan-cancer genetic analysis identifies PARK2 as a master regulator of G1/S cyclins. Nat Genet. 2014; 46(6):588–594. [PubMed: 24793136]
43. Zhang C, Lin M, Wu R, et al. Parkin, a p53 target gene, mediates the role of p53 in glucose metabolism and the Warburg effect. Proc Natl Acad Sci U S A. 2011; 108(39):16259–16264. [PubMed: 21930938]
44. Viotti J, Duplan E, Caillava C, et al. Glioma tumor grade correlates with parkin depletion in mutant p53-linked tumors and results from loss of function of p53 transcriptional activity. Oncogene. 2014; 33(14):1764–1775. [PubMed: 23644658]
45. Sarraf SA, Raman M, Guarani-Pereira V, et al. Landscape of the PARKIN-dependent ubiquitylome in response to mitochondrial depolarization. Nature. 2013; 496(7445):372–376. [PubMed: 23503661]
46. Narendra D, Tanaka A, Suen DF, Youle RJ. Parkin is recruited selectively to impaired mitochondria and promotes their autophagy. J Cell Biol. 2008; 183(5):795–803. [PubMed: 19029340]
47. Beilina A, Van Der Brug M, Ahmad R, et al. Mutations in PTEN-induced putative kinase 1 associated with recessive parkinsonism have differential effects on protein stability. Proc Natl Acad Sci U S A. 2005; 102(16):5703–5708. [PubMed: 15824318]
48. Sammarco MC, Grabczyk E. A series of bidirectional tetracycline-inducible promoters provides coordinated protein expression. Anal Biochem. 2005; 346(2):210–216. [PubMed: 16212928]
49. Suganya R, Chakraborty A, Miriyala S, Hazra TK, Izumi T. Suppression of oxidative phosphorylation in mouse embryonic fibroblast cells deficient in apurinic/apyrimidinic endonuclease. DNA Repair (Amst). 2015; 27C:40–48.
50. Collett MS, Erikson RL. Protein kinase activity associated with the avian sarcoma virus src gene product. Proc Natl Acad Sci U S A. 1978; 75(4):2021–2024. [PubMed: 205879]
51. Izumi T, Malecki J, Chaudhry MA, et al. Intragenic suppression of an active site mutation in the human apurinic/apyrimidinic endonuclease. J Mol Biol. 1999; 287(1):47–57. [PubMed: 10074406]
52. Scheffner M, Werness BA, Huibregtse JM, Levine AJ, Howley PM. The E6 oncoprotein encoded by human papillomavirus types 16 and 18 promotes the degradation of p53. Cell. 1990; 63(6): 1129–1136. [PubMed: 2175676]
53. Marchenko ND, Wolff S, Erster S, Becker K, Moll UM. Monoubiquitylation promotes mitochondrial p53 translocation. EMBO J. 2007; 26(4):923–934. [PubMed: 17268548]
54. Lee KY, Myung K. PCNA modifications for regulation of post-replication repair pathways. Mol Cells. 2008; 26(1):5–11. [PubMed: 18525240]

55. Chung KK, Zhang Y, Lim KL, et al. Parkin ubiquitinates the alpha-synuclein-interacting protein, synphilin-1: implications for Lewy-body formation in Parkinson disease. Nat Med. 2001; 7(10): 1144–1150. [PubMed: 11590439]
56. Wang HL, Chou AH, Wu AS, et al. PARK6 PINK1 mutants are defective in maintaining mitochondrial membrane potential and inhibiting ROS formation of substantia nigra dopaminergic neurons. Biochim Biophys Acta. 2011; 1812(6):674–684. [PubMed: 21421046]
57. Haque ME, Thomas KJ, D'Souza C, et al. Cytoplasmic Pink1 activity protects neurons from dopaminergic neurotoxin MPTP. Proc Natl Acad Sci U S A. 2008; 105(5):1716–1721. [PubMed: 18218782]
58. Hegde ML, Banerjee S, Hegde PM, et al. Enhancement of NEIL1 protein-initiated oxidized DNA base excision repair by heterogeneous nuclear ribonucleoprotein U (hnRNP-U) via direct interaction. J Biol Chem. 2012; 287(41):34202–34211. [PubMed: 22902625]
59. Joo JH, Dorsey FC, Joshi A, et al. Hsp90-Cdc37 chaperone complex regulates Ulk1- and Atg13-mediated mitophagy. Mol Cell. 2011; 43(4):572–585. [PubMed: 21855797]
60. Tanaka A. Parkin-mediated selective mitochondrial autophagy, mitophagy: Parkin purges damaged organelles from the vital mitochondrial network. FEBS Lett. 2010; 584(7):1386–1392. [PubMed: 20188730]
61. Lazarou M, Jin SM, Kane LA, Youle RJ. Role of PINK1 binding to the TOM complex and alternate intracellular membranes in recruitment and activation of the E3 ligase Parkin. Dev Cell. 2012; 22(2):320–333. [PubMed: 22280891]
62. Narendra DP, Jin SM, Tanaka A, et al. PINK1 is selectively stabilized on impaired mitochondria to activate Parkin. PLoS Biol. 2010; 8(1):e1000298. [PubMed: 20126261]
63. Brooks J, Ding J, Simon-Sanchez J, Paisan-Ruiz C, Singleton AB, Scholz SW. Parkin and PINK1 mutations in early-onset Parkinson's disease: comprehensive screening in publicly available cases and control. J Med Genet. 2009; 46(6):375–381. [PubMed: 19351622]
64. Beasley SA, Hristova VA, Shaw GS. Structure of the Parkin in-between-ring domain provides insights for E3-ligase dysfunction in autosomal recessive Parkinson's disease. Proc Natl Acad Sci U S A. 2007; 104(9):3095–3100. [PubMed: 17360614]
65. Wenzel DM, Lissounov A, Brzovic PS, Klevit RE. UBCH7 reactivity profile reveals parkin and HHARI to be RING/HECT hybrids. Nature. 2011; 474(7349):105–108. [PubMed: 21532592]
66. Frossi B, Tell G, Spessotto P, Colombatti A, Vitale G, Pucillo C. H(2)O(2) induces translocation of APE/Ref-1 to mitochondria in the Raji B-cell line. J Cell Physiol. 2002; 193(2):180–186. [PubMed: 12384995]
67. Wu SN, Jan CR, Li HF. Ruthenium red-mediated inhibition of large-conductance Ca2+-activated K + channels in rat pituitary GH3 cells. J Pharmacol Exp Ther. 1999; 290(3):998–1005. [PubMed: 10454470]
68. Shimura H, Hattori N, Kubo S, et al. Familial Parkinson disease gene product, parkin, is a ubiquitin-protein ligase. Nat Genet. 2000; 25(3):302–305. [PubMed: 10888878]
69. Zhang Y, Gao J, Chung KK, Huang H, Dawson VL, Dawson TM. Parkin functions as an E2-dependent ubiquitin- protein ligase and promotes the degradation of the synaptic vesicle-associated protein, CDCrel-1. Proc Natl Acad Sci U S A. 2000; 97(24):13354–13359. [PubMed: 11078524]
70. Nicolini G, Miloso M, Zoia C, Di Silvestro A, Cavaletti G, Tredici G. Retinoic acid differentiated SH-SY5Y human neuroblastoma cells: an in vitro model to assess drug neurotoxicity. Anticancer Res. 1998; 18(4A):2477–2481. [PubMed: 9703895]
71. Kelley MR, Georgiadis MM, Fishel ML. APE1/Ref-1 role in redox signaling: translational applications of targeting the redox function of the DNA repair/redox protein APE1/Ref-1. Curr Mol Pharmacol. 2012; 5(1):36–53. [PubMed: 22122463]
72. Gorman MA, Morera S, Rothwell DG, et al. The crystal structure of the human DNA repair endonuclease HAP1 suggests the recognition of extra-helical deoxyribose at DNA abasic sites. EMBO J. 1997; 16(21):6548–6558. [PubMed: 9351835]
73. Izumi T, Mitra S. Deletion analysis of human AP-endonuclease: minimum sequence required for the endonuclease activity. Carcinogenesis. 1998; 19(3):525–527. [PubMed: 9525290]

74. Fantini D, Vascotto C, Marasco D, et al. Critical lysine residues within the overlooked N-terminal domain of human APE1 regulate its biological functions. Nucleic Acids Res. 2010; 38(22):8239–8256. [PubMed: 20699270]

75. Fiszer-Kierzkowska A, Vydra N, Wysocka-Wycisk A, et al. Liposome-based DNA carriers may induce cellular stress response and change gene expression pattern in transfected cells. BMC Mol Biol. 2011; 12:27. [PubMed: 21663599]

76. Jacobsen L, Calvin S, Lobenhofer E. Transcriptional effects of transfection: the potential for misinterpretation of gene expression data generated from transiently transfected cells. BioTechniques. 2009; 47(1):617–624. [PubMed: 19594446]

77. Szczesny B, Mitra S. Effect of aging on intracellular distribution of abasic (AP) endonuclease 1 in the mouse liver. Mech Ageing Dev. 2005; 126(10):1071–1078. [PubMed: 15951004]

78. Mitra S, Izumi T, Boldogh I, Bhakat KK, Chattopadhyay R, Szczesny B. Intracellular trafficking and regulation of mammalian AP-endonuclease 1 (APE1), an essential DNA repair protein. DNA Repair (Amst). 2007; 6(4):461–469. [PubMed: 17166779]

79. Wu HH, Cheng YW, Chang JT, et al. Subcellular localization of apurinic endonuclease 1 promotes lung tumor aggressiveness via NF-kappaB activation. Oncogene. 2010; 29(30):4330–4340. [PubMed: 20498636]

80. Li M, Zhong Z, Zhu J, et al. Identification and characterization of mitochondrial targeting sequence of human apurinic/apyrimidinic endonuclease 1. J Biol Chem. 2010; 285(20):14871–14881. [PubMed: 20231292]

81. Kakolyris S, Kaklamanis L, Giatromanolaki A, et al. Expression and subcellular localization of human AP endonuclease 1 (HAP1/Ref-1) protein: a basis for its role in human disease. Histopathology. 1998; 33(6):561–569. [PubMed: 9870152]

82. Vascotto C, Bisetto E, Li M, et al. Knock-in reconstitution studies reveal an unexpected role of Cys-65 in regulating APE1/Ref-1 subcellular trafficking and function. Mol Biol Cell. 2011; 22(20):3887–3901. [PubMed: 21865600]

83. Hu HH, Kannengiesser C, Lesage S, et al. PARKIN Inactivation Links Parkinson's Disease to Melanoma. J Natl Cancer Inst. 2016; 108(3)

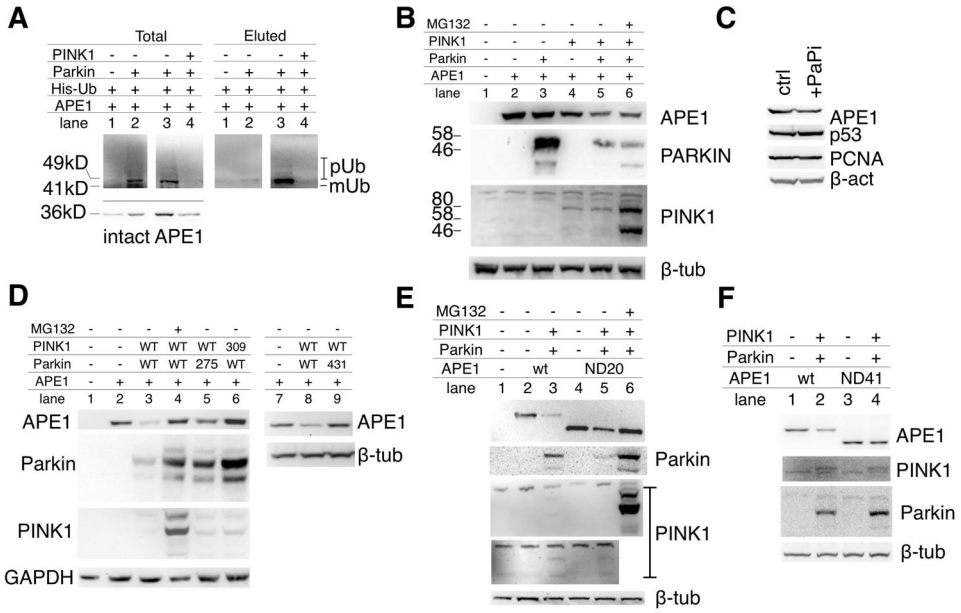

Fig. 1. Functional requirements for APE1 ubiquitination

(**A**) Detection of monoubiquitinated and polyubiquitinated APE1. A549 was transfected with APE1 and His-tagged Ubiquitin (His-Ub) along with vector control (lane 1), Parkin (lanes 2 and 3), Parkin and PINK1 (lane 4). Total protein lysates and eluted fractions (enriched with His-Ub) were analyzed with APE1 antibody as described in Materials and Methods. (**B**) MEF^{la} transfected with 1: vector control, 2: APE1, 3: APE1 and Parkin, 4: APE1 and PINK1, 5: APE1, PINK1, and PARKIN, 6: APE1, PINK1, PARKIN with 10 μM MG132 for 6 h. (**C**) MEF^{la} transfected with APE1, PCNA, p53 without (ctrl) or with Parkin and PINK1 (PaPi) and the stabilities of APE1, PCNA, p53 were monitored after 24 h. (**D**) Wild-type (WT) or mutant Parkin (275 = R275W, 431 = C431F) and PINK1 (309 = G309D) were co-transfected in MEF^{la} as shown in the table. Protein levels were examined after 24 h incubation. MG132 was at 3 μM for 16 h. (**E**) The WT (full-length) or ND20 (N-terminal 20 a.a. truncation) APE1 was co-transfected with Parkin and PINK1 in MEF^{la}. Lane 6: MG132 was added at 3 μM for overnight incubation. Expression of PINK1 in lanes 3 and 5 was confirmed separately from lane 6 which otherwise caused a halo effect. (**F**) ND41 (41 a.a. N-terminal truncation) APE1 was examined after Parkin and PINK1 expression.

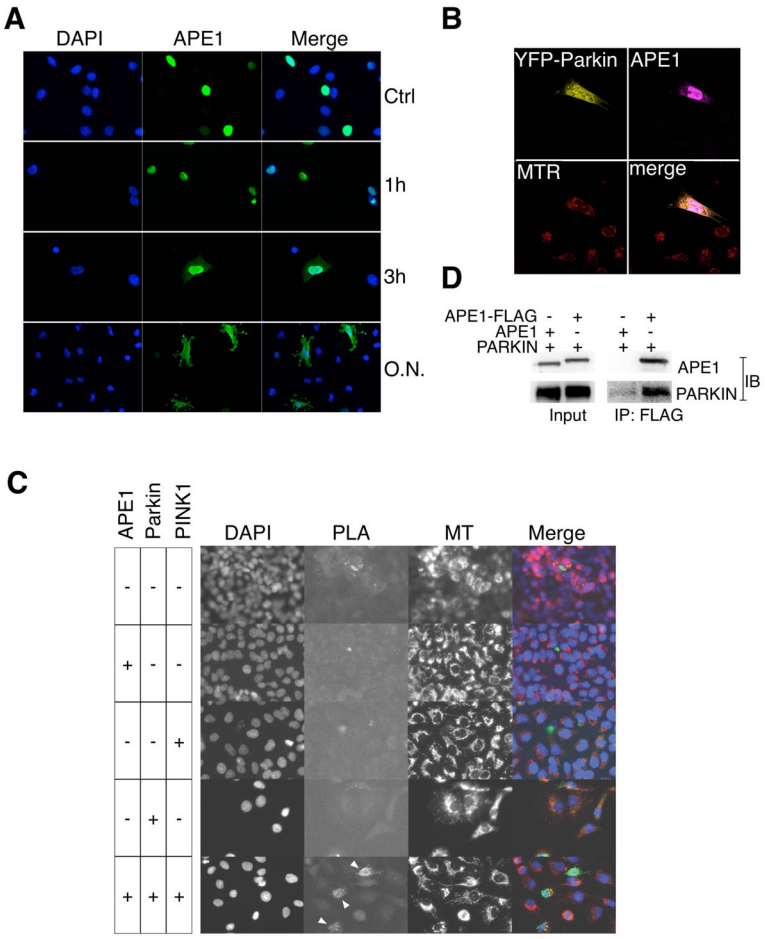

Fig. 2. Interaction of APE1 with Parkin in the cytoplasm

(**A**) Accumulation of APE1 in the presence of MG132. MEF^{la} cells expressing the wild-type APE1 were incubated with MG132 for indicated time periods. MG132 concentrations were 40 μM (0 – 3 h) and 3 μM (overnight). APE1 was labeled with anti-APE1 antibody and AlexaFluor 488 and analyzed in fluorescence microscopy. (**B**) MEF^{la} transfected with APE1 and YFP-Parkin were incubated with MG132 40 μM for 3 h, fixed, labeled with anti-APE1 and AlexaFluor 633 (shown in purple), and then analyzed by confocal microscopy. Red: MitoTracker Red, Green: YFP-Parkin, Blue: APE1, X: Merged. Z-series pictures were taken for a detailed analysis (Fig. S3). (**C**) Proximity ligation assay (PLA) between APE1 and Parkin in A549. A549 expressing APE1, Parkin, PINK1 as indicated. APE1 and Parkin specific antibodies were used to probe the interactions of the two proteins as described in Materials and Methods. Positive signals were seen only in the cells co-transfected with APE1, Parkin, PINK1 (bottom panel shown with arrows). MT: fluorescent signals by MitoTracker Red (Invitrogen). (**D**) Co-immunoprecipitation of APE1 and Parkin. Parkin and APE1 (lane 1) or Parkin and APE1-FLAG (lane 2) co-expressed in *E. coli* BLR were subjected to immunoprecipitation using FLAG antibody, and the total and eluted fractions were analyzed in immunoblot using APE1 and Parkin antibodies.

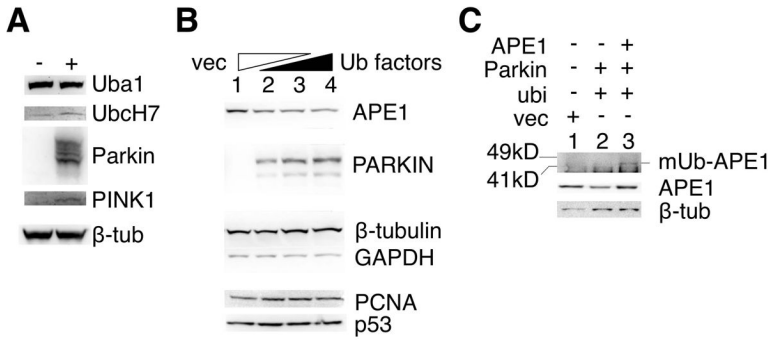

Fig. 3. Parkin targets endogenous APE1 for degradation

(**A**) Expression of Parkin and its cofactors, Uba1, UbcH7, Parkin and PINK1 in A549. A549 was transfected with (−) empty vector alone or (+) the vectors carrying Parkin, PINK1, Uba1, and UbcH7 cDNAs. β-tub: β-tubulin. Note that there was no change in the Uba1 probably due to its abundance. (**B**) A549 cells were transfected with cDNA expression vectors for ubiquitin, UBA1, UBCH7, Parkin, PINK1. Amount of each DNA: 1: 0 μg, 2: 0.17 μg, 3: 0.35 μg, 4: 0.7 μg. Empty vector DNA (vec) was added to each to make the total amount of DNA equal among samples. Cells were then incubated for 16 h, and harvested for immunoblot examination. (**C**) A549 transfected with vector alone (1) or ubiquitin, Uba1, UbcH7, Parkin and PINK1 as in (B) and incubated with MG132 (3 μM for 16 h), and APE1 (middle) and its ubiquitinated forms (top), as well as β-tubulin (bottom) were analyzed by immunoblot separately.

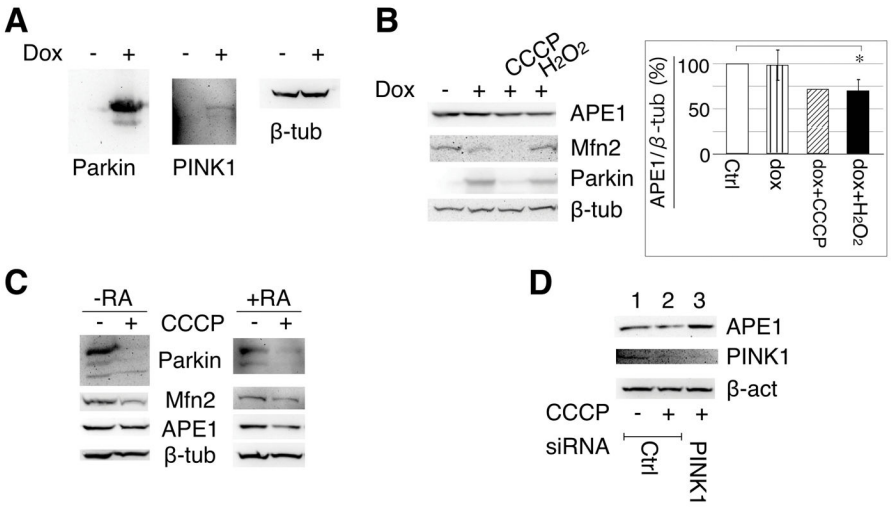

Fig. 4. Effect of Parkin and PINK1 co-expression on endogenous APE1

(**A**) Parkin and PINK1 expressions examined in 293-PaPi cell lysates after 16 h treatment without (lane 1) or with (lane 2) dox (2 μg/mL). (**B**) (Left) Immunoblot for APE1, Parkin, Mfn2, and β-tubulin levels in 293-PaPi cells treated with dox for 16 h. CCCP: 10 μM; H_2O_2: 50 μM. (Right) Averages of APE1/β-tubulin ratios with the treatments as indicated. *$p <$ 0.05. (**C**) SH-SY5Y cells were incubated with DMSO only (−) or with 10 μM CCCP (+), and incubated for 24 h at 37°C and analyzed by immunoblot. In the right panel, SH-SY5Y cells were differentiated by the 5-days treatment with 10 μM retinoic acid (RA), and then incubated with 10 μM CCCP for 24 h. (**D**) Scrambled control (lanes 1 and 2) or PINK1 siRNA (lane 3) were electroporated in SH-SY5Y, and the level of APE1 was examined after 72 h incubation with 24 h treatment of DMSO (lanes 1 and 3) or 10 μM CCCP (lane 2).

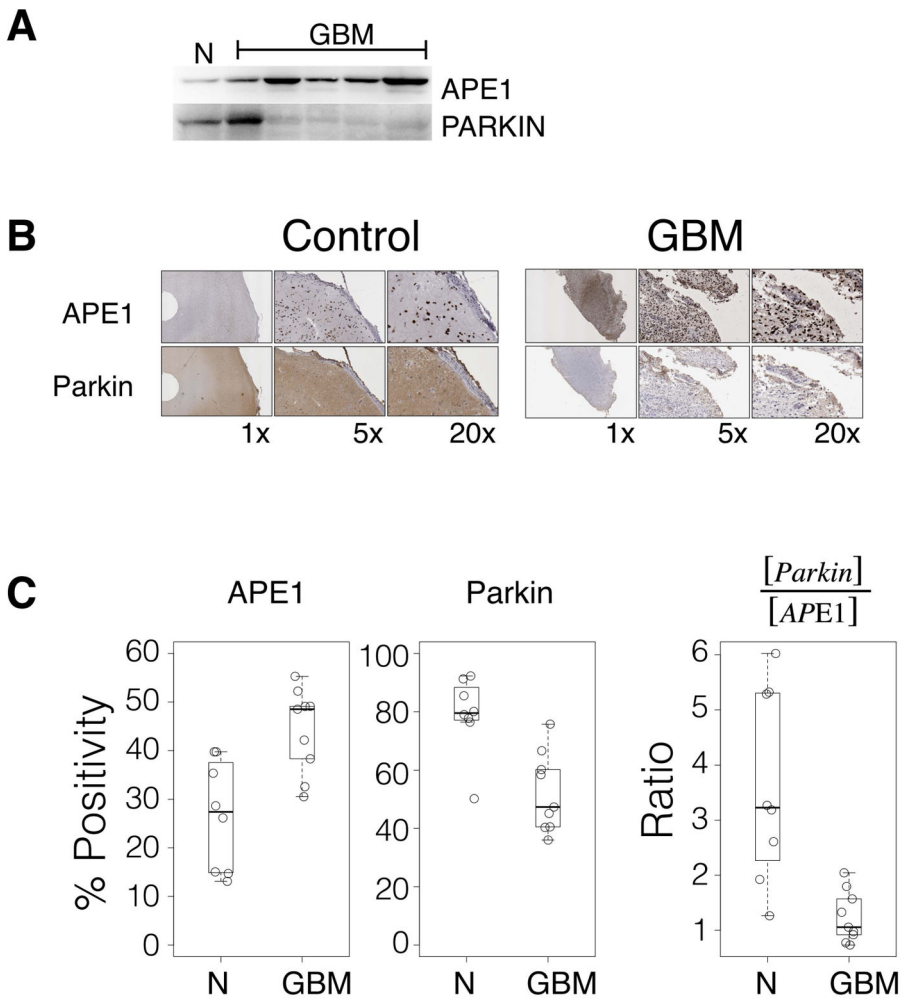

Fig. 5. Parkin and APE1 expressions in GBM

(**A**) Five glioma and one non-neoplasic (from epilepsy surgery) brain tissues were processed for protein extraction and analyzed in immunoblot assays. (B) Representative results of immunohistochemistry from non-neoplastic (Control) and GBM tissues. Magnifications: 1x, 5x, and 20x. (**C**) Total levels of APE1 (**Left** panel) and Parkin (**Middle** panel) were measured and normalized by nuclear counts using Aperio analytical software (Leica), and are shown as box plots for the non-neoplastic (N) and GBM brain tissues. (**Right** panel) Parkin levels were divided by APE1 levels of the corresponding tissues, and the calculated ratios are plotted. Each box plot shows the median value (bold horizontal line), the first and third quartile (box), and 1.5 x interquartile range (whiskers). Individual values are also shown as circles. The p values (Student's t-test) are 0.009, 0.0025, 0.0013 for the left, middle, and the right panel, respectively.

Table 1

Effect of Parkin and PINK1 on the stability of APE1[a].

APE1	Parkin	PINK1	Decrease (%)[b]	p[c]
WT	WT	WT	46.0 ± 18.0	-
ND21	WT	WT	42.9 ± 7.5	0.63
ND41	WT	WT	83.4 ± 24.4	0.008
WT	R275W	WT	81.7 ± 5.90	< 0.001
WT	C431F	WT	109.0 ± 12.03	< 0.001
WT	WT	G309D	96.17 ± 31.0	< 0.001
WT	WT	-	97.3	
WT	-	WT	84	

[a] Relative APE1 intensities (%) in MEF[la] with the wild-type or mutant Parkin and PINK1 expressions were calculated by comparing with those without Parkin nor PINK1.

[b] APE1 amounts were normalized by β-tubulin, and compared with that without Parkin and PINK1. Values based on more than three independent experiments.

[c] P values by Student's t-test. Each value (more than three experiments) calculated with the result of the first row (with wt-APE1, wt-Parkin, and wt-PINK1).